12.2 3D Gesture-Sensing System for Interactive Displays Based on Extended-Range Capacitive Sensing

Yingzhe Hu, Liechao Huang, Warren Rieutort-Louis, Josue Sanz-Robinson, Sigurd Wagner, James C. Sturm, Naveen Verma

Princeton University, Princeton, NJ

Capacitive touch screens have enabled compelling interfaces for displays [1]. Three-dimensional (3D) sensing, where user gestures can also be sensed in the out-of-plane dimension to distances of 20 to 30cm, represents new interfacing possibilities that could substantially enrich user experience. The challenge is achieving sensitivity at these distances when sensing the small capacitive perturbations caused by user interaction with sensing electrodes. Among capacitive-sensing approaches, self capacitance enables substantially greater distance than mutual capacitance (i.e., between electrodes), but can suffer from ghost effects during multi-touch. For gesture recognition, however, processing via classifiers can overcome such effects, enabling a rich dictionary of gestures [2]. Nonetheless, the sensing distance of such systems has been too limited for 3D sensing.

In this work, we present a 3D sensing system with 40×40cm^2 area and sensing distance to 30cm. This distance is achieved via two approaches. First, capacitance sensing is performed via frequency modulation, and the sensitivity of frequency readout is enhanced by high-Q oscillators capable of filtering noise sources in the readout system as well as stray noise sources from display coupling. Second, the capacitance signal is enhanced by eliminating electrostatic coupling between the sensing electrodes and surrounding ground planes. Figure 12.2.1 illustrates the concept. As shown on top, in order to minimize display thickness, ITO sensing electrodes are integrated with increasingly minimal separation to the display's common-electrode plane. This gives large electrostatic coupling from the sensing electrodes to the display, substantially degrading the coupling achievable to a user at a distance. In this system, however, the sensing electrodes are isolated from the display's common electrode by an ITO oscillating plane (OP). As shown, the sensing electrodes are connected one-by-one to a sensing LC oscillator (SO), such that their self-capacitance perturbs the tank capacitance, causing a frequency shift. Meanwhile, the OP is driven to the same voltage as the SO (and hence the connected electrode) by a unity-gain buffer (source follower). Consequently, electric field due to oscillatory charge redistribution on the electrode does not interact with the OP, resulting in much stronger coupling to a user even at great distances. In addition to sensing distance, this enables several benefits. First, since coupling between the electrodes and the OP is not a factor, their separation distance can be aggressively reduced (<1mm is used in this work). Second, separation between the OP and the display common electrode can also be reduced at the cost of increased OP capacitance and thus higher power in the unity-gain buffer; however, the OP driver consumes less than 19mW in this work with a separation of 1mm, making its overhead acceptable. A benefit of frequency-modulated readout is also that minimal noise is imposed on the display since the amplitude is not critical for increasing distance and is thus fixed at a value (0.75V). Third, extended sensing distance enables electrodes to provide later-displacement information (characterized below), allowing fewer electrode channels for covering large display areas, thus significantly mitigating power consumption and scan-rate constraints.

Figure 12.2.2 shows the readout channel architecture. Scanning of the sensing electrodes is controlled by a shift register. The SO's nominal center frequency of f_C=5MHz (tunable via MOS varactor) is perturbed by an amount Δf due to the sensed capacitance. The SO output is then fed to a differential Gilbert mixer and modulated down using a fixed local oscillator (LO). A low-frequency output f_{SENSE} is then derived from low-pass filtering (via a 2nd-order filter). The nominal SO and LO frequencies are offset by f_{OFFSET} (tunable by varactor) to give a minimum f_{SENSE}, which sets both the maximum output range of the time-to-digital converter (TDC) as well as the maximum scan rate. In this design f_{OFFSET} can be set from 5 to 20kHz. f_{SENSE} is amplified via a 2-stage preamp and a comparator before being provided to the TDC. The resulting digital signal controls an enable signal EN for a 16b counter through a period-control block. Since f_{SENSE} is a fairly non-linear function over sensing distance, the period-control block helps address TDC dynamic range by allowing multiples of the f_{SENSE} period to be selected for the counter EN signal; when f_{SENSE} is at high frequencies (due to short sensing distances), multiples N=2,4,8,16 can be selected. Such cases can be determined from the TDC code, and a digital controller can readily respond since high f_{SENSE} frequencies correspond to reduced readout delay. The sensed frequency shift, for a TDC count C, is thus $\Delta f = N \times f_C/C - f_{OFFSET}$. Readout noise is a key factor affecting sensitivity and is dominated by the SO/LO, mixer, and preamp, as discussed below.

Figure 12.2.3 shows the SO (LO has same structure) and mixer. Oscillator phase noise is a critical aspect and is set by device noise (1/f and white) as well as stray coupling from the display. Low phase noise is achieved thanks to substantial filtering of all these sources provided by the tank [3]. This requires high tank quality factor (Q), primarily limited by the inductor. We use an 0805 inductor of 33μH, giving Q=400 at 5MHz. In addition to tank Q, biasing-current noise is also a critical factor. We add a 100pF capacitor at the drain of the tail device, and also set the tail-current magnitude to ensure current-limiting, rather than voltage-limiting, conditions [3], giving a phase noise improvement of 21dB (@100Hz from f_C). Mixer linearity is also a critical factor for sensitivity. Since the SO and LO frequencies are offset, harmonics raise the possibility of in-band beat frequencies in the output at multiples of the ideal f_{SENSE}. To mitigate non-linearity, the SO is provided via a capacitor divider, as shown, to reduce its swing to ~100mV. The low-pass filter following the mixer has cut-off frequency of 50kHz to filter high frequencies and mixer clock feed through.

Figure 12.2.4 shows the preamp and comparator. With f_{SENSE} modulated to a low frequency, amplitude noise with respect to a zero-crossing reference can substantially degrade sensitivity, causing noise in the TDC output. To mitigate amplitude noise, the 2-stage preamp with diode-connected PMOS loads provides 6× gain per stage with noise filtering at a cutoff frequency of 200kHz per stage, set by 5pF output capacitors. The preamp feeds a hysteretic comparator. Hysteresis is adopted to ensure a digital output free of transient glitches, which is important for the operation of the TDC period-control block. The total input-referred noise of the mixer, preamp and comparator stages is 1.4μV_{RMS}, corresponding to a frequency readout noise of σ_f=16Hz$_{RMS}$.

The system is prototyped, with the frequency-readout IC implemented in a 0.13μm CMOS process from IBM, and the sensing electrodes and OP patterned in-house using ITO-clad PET. The sensing electrodes are 1cm wide and spaced with 10cm pitch. For testing, we use 4 channels in each of the X and Y dimensions (8 channels total), giving a sensing area of 40×40cm^2. Figure 12.2.5 shows sensitivity measurements. On the left, the readout SNR and TDC code (with RMS bars) is plotted versus distance for a finger positioned above a sensing electrode; as shown substantial SNR is maintained out to 30cm (with 30dB SNR at 16cm). Though SNR is a widely used metric, in fact it is not representative of sensitivity in the presence of stray noise, such as from the display. On the right, we show the TDC code (with RMS bars) when display noise, varied from zero to various peak-peak values, is driven directly onto the OP (by a capacitively coupled amplifier whose input is fed from a display's common electrode); minimal impact on readout is observed even with large noise values. Figure 12.2.6 shows the measurement summary and a comparison with the state of the art. While other systems are touch-based, the presented system achieves the highest reported SNR for distances to 30cm. As an example, the worst-case resolution for lateral-displacement sensing is shown at 20cm above the electrode (resolution is defined as the displacement at which the difference in mean TDC code equals the code RMS). The digital circuits and OP driver are powered from 1.2V while the analog circuits are powered from 2.5V, giving total power consumption less than 20mW (475μW for frequency readout, 19mW for OP driver). The readout time is 500μs per channel, enabling a 240Hz scan rate.

Acknowledgements:
This work is funded by the Qualcomm Innovation Fellowship and NSF (grants ECCS-1202168 and CCF-1218206). We also thank MOSIS for IC fabrication.

References:
[1] H.-R. Kim, *et al.*, "A Mobile-Display-Driver IC Embedding a Capacitive Touch-Screen Controller System," *ISSCC Dig. Tech. Papers*, pp. 114-115, Feb. 2010.
[2] Zytronic. http://www.zytronic.co.uk/news/white-papers/. (online).
[3] A. Hajimiri and T H. Lee, "Design Issues in CMOS Differential LC Oscillators," *IEEE J. Solid-State Circuits*, vol. 34, no. 5, pp. 717-724, May 1999.

 978-1-4799-0920-9/14/$31.00

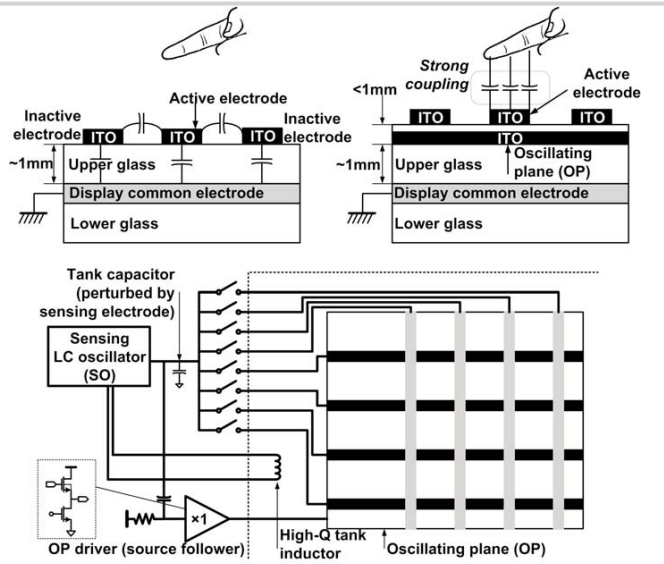

Figure 12.2.1: 3D gesture-sensing system architecture.

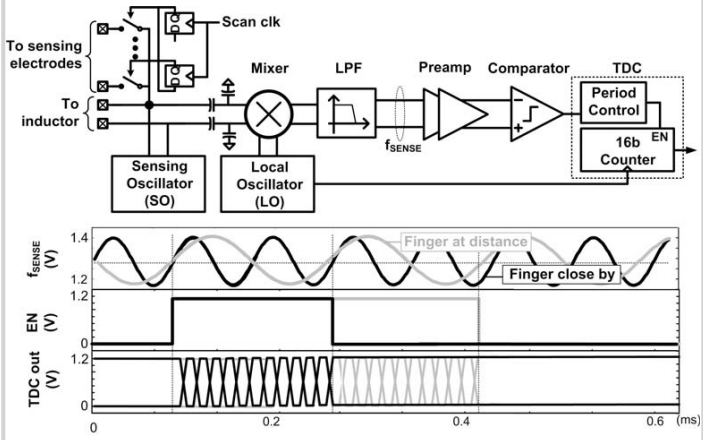

Figure 12.2.2: Frequency-modulation readout system based on low-noise oscillators and TDC; simulation waveforms illustrate frequency-modulation response by system for finger close by and at distance.

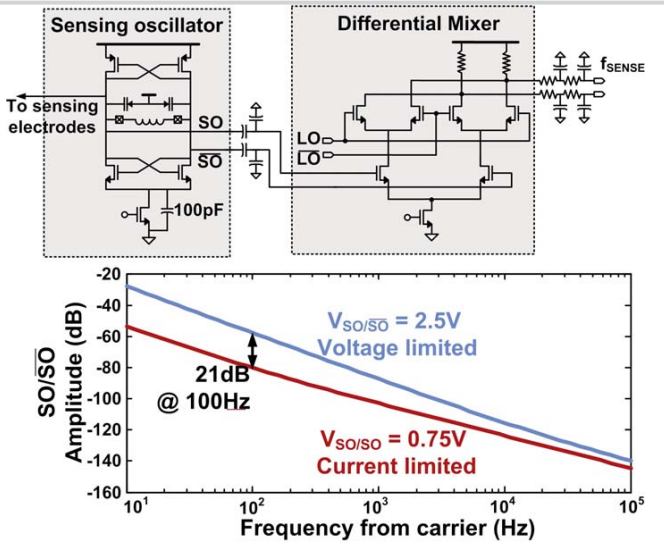

Figure 12.2.3: Sensing oscillator (SO) and mixer; oscillator phase noise is compared for current- versus voltage-limiting conditions.

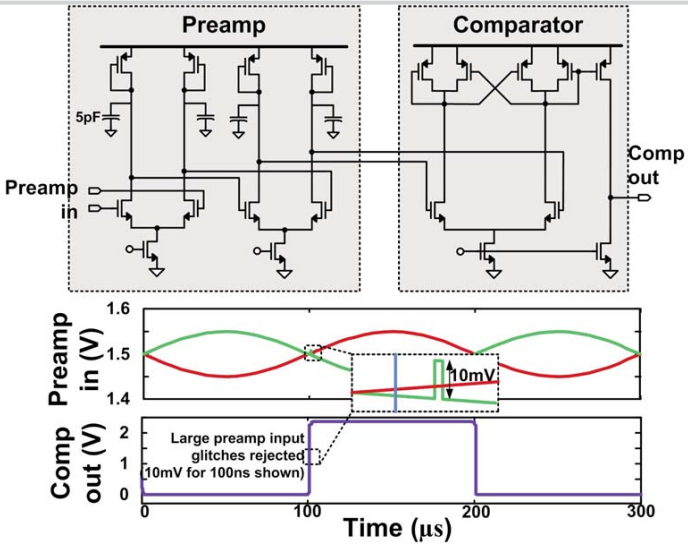

Figure 12.2.4: Preamp and comparator for generating digital TDC input from f_{SENSE}; glitch-free output is achieved with hysteretic comparator.

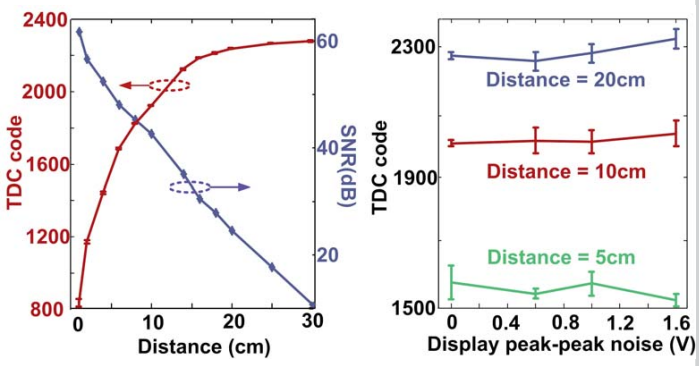

Figure 12.2.5: Prototype sensitivity measurements, showing SNR and TDC code (with RMS bars) versus distance (out to 30cm) as well as TDC code error due to stray coupling of display noise with varying peak-peak noise applied to oscillating plane.

	H.-R. Kim ISSCC10	K.-D. Kim ISSCC12	J.-H. Yang ISSCC13	This work
Process	1.5/5.5/30V 90nm CMOS	1.5/5.5/30V 90nm LDI	3.3V 350nm CMOS	1.2/2.5V 130nm CMOS
Channels	24 (X+Y)	30 (X+Y)	Tx 27; Rx 43	8 (X+Y)
Panel size	6.5cm x 4.9cm	6.5cm x 4.9cm	20.5cm x 15.4cm	40cm x 40cm
3D sensing	X	X	X	To 30cm
Capacitance type	Self capacitance	Self capacitance	Mutual capacitance	Self capacitance
Scan frequency	120Hz	120Hz	120Hz	240Hz
SNR	30dB	35dB	39dB	50dB@5cm 30dB@16cm 20dB@23cm
Resolution	--	0.9mm†	--	7.1mm(x) 7.1mm(y) 10mm(z)@20cm(hand)
Power consumption	12mW	10.6mW	18.7mW	210µW (readout) 19mW (OP)

†Precise definition of resolution not available

Figure 12.2.6: Performance summary and comparison with the state of the art.

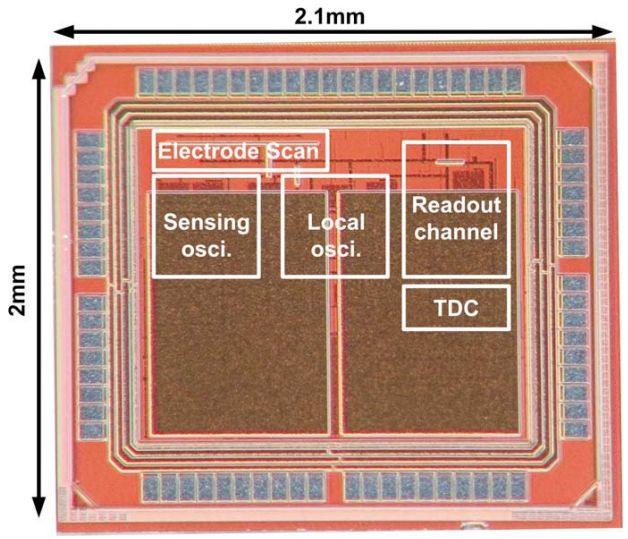

Figure 12.2.7: Die photo of prototype IC implemented in 0.13µm CMOS process from IBM.

978-1-4799-0920-9/14/$31.00